Dynamic grating recording in semiconductor CdF_2:Ga,Y

Y. Uesu, K. Yasukawa, N. Saito, and S. Itoh

Department of Physics, Waseda University, 3-4-1 Okubo, Shinjuku-ku, Tokyo 169-8555, Japan

S. Odoulov and K. Shcherbin

Institute of Physics, National Academy of Sciences, 03650, Kiev-39, Ukraine

A. I. Ryskin

S. I. Vavilov State Optical Institute, 199034 St. Petersburg, Russia

Received October 28, 2002; revised manuscript received April 29, 2003

Cadmium fluoride codoped with Ga and Y is characterized as a medium for phase grating recording. The dependence of the three-dimensional grating diffraction efficiency on the intensity of the recording light, on the polarization of the recording light, on the fringe contrast, and on the spatial frequency of the fringe was measured together with the dynamic characteristics (grating decay time and grating buildup time). The crystal behaves as a $\chi^{(3)}$ medium with its refractive-index change depending on linear intensity and with nearly exponential buildup–decay temporal characteristics for moderate intensities of the green recording light at room temperature.

OCIS codes: 190.4720, 210.4810, 090.2900, 090.7330.

1. INTRODUCTION

Cadmium fluoride doped with Ga or In impurities after annealing in a reduction atmosphere becomes a semiconductor and manifests highly sensitive light-induced conversion of the bistable DX centers (see, for instance, Refs. 1 and 2). This conversion is accompanied by strong variation in the absorption spectrum and by considerable changes (as much as 10^{-4}) of the refractive index for visible light. Their large index variation makes these crystals potential candidates for optical information recording and processing.[3–6] At temperatures lower than 240 K the light-induced index variation for CdF_2:Ga is stable in time and can be erased by heating. This fact indicates that the material is suitable for use in information retrieval and storage.[3] It was shown recently[5,6] that at ambient temperature the lifetime of the light-induced state of a deep center decreases dramatically, which allows this material to be considered a medium for real-time holography. The publications cited above[5,6] are devoted mainly to the development and justification of a microscopic model of light-induced excitation of the metastable state of the deep DX center and its thermal decay. In present paper we study the properties of cadmium fluoride, both static and dynamic, that characterize this crystal as a recording medium for dynamic holography at room temperature.[7] The complimentary *Z*-scan technique[8] is used for determination of the sign of a nonlinear optical constant.

2. EXPERIMENTS

A. Experimental Procedure

A CdF_2:Ga, Y single crystal was grown by the Stockbarger–Bridgeman technique. Dopants were added to the raw material. Codoping with Y was done to improve the optical quality of the crystal and to increase the Ga content.[9] The concentration of the active Ga centers was $1.7 \times 10^{18}\,\mathrm{cm}^3$. After being heated in a reducing atmosphere of K and Cd vapors, the samples became photosensitive. They had a slightly greenish color, with absorption coefficient $\alpha \approx 0.7\ \mathrm{cm}^{-1}$ at $\lambda = 0.53\ \mu\mathrm{m}$. With a linear index of refraction $n \approx 1.6$, Fresnel reflection constant R for small incidence angle was not too high, i.e., $R \approx 0.05$.

CdF_2 belongs to cubic symmetry class $m-3m$; it is therefore optically isotropic and does not feature optical activity. A sample with dimensions 7 mm × 3 mm × 4 mm was cut along the crystallographic axes {100}, {010}, and {001} and had two optically finished faces with 4-mm spacing between them. Two light beams from a cw frequency-doubled Nd^{3+}:YAG laser (single mode; single frequency; output power, 100 mW) entered the sample as shown in Fig. 1A. Because of the considerable divergence of the green laser beam the illuminated area on the sample input face had a diameter of ~3 mm ($1/e^2$ intensity level in a Gaussian distribution).

A polarization beam splitter and a phase retarder in front of it were used to control the intensity ratio of two

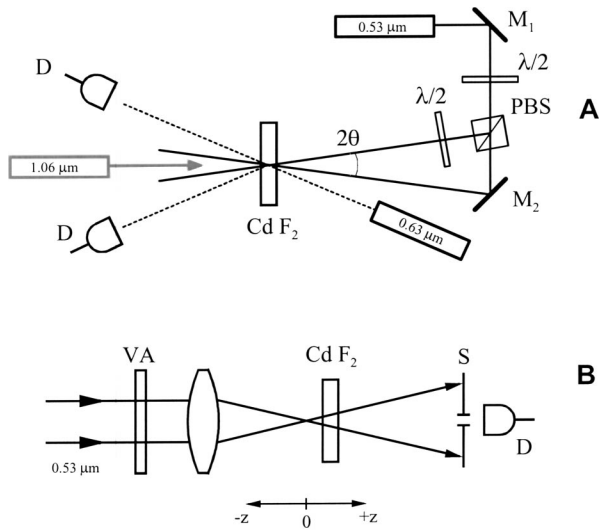

Fig. 1. Experimental setups for A, the holographic experiment and B, the *Z*-scan experiment: Ms, mirrors; PBS, polarization beam splitter; λ/2's, phase retarders; VA, variable attenuator; S, screen with an aperture; Ds, photodetectors. The recording was done with the green light of a cw frequency-doubled Nd^{3+}:YAG laser, whereas the red light of a He–Ne laser was used for readout. In some experiments the near-infrared radiation of a Nd^{3+}:YAG laser was sent to the sample during recording.

recording beams. A second phase retarder was put in one of the two recording beams to rotate the polarization by 90°. In this way the two recording beams were polarized parallel to each other. One extra light beam from the red He–Ne laser entered the sample surface at the appropriate Bragg angle; the diameter of this beam was ~1 mm, i.e., three times smaller than the diameter of the recording beams. As the power of the red laser beam was less than 1 mW, the readout process can be considered nondestructive. The intensities of transmitted (I_t) and diffracted (I_d) red beams were measured at room temperature with photodetectors, and the diffraction efficiency η was determined:

$$\eta = \frac{I_d}{I_t + I_d}. \tag{1}$$

With this definition, the losses that were due to Fresnel reflections on the sample faces and the attenuation of the diffracted beam that was due to crystal absorption were excluded automatically.

In a separate experiment, the self-action of the focused laser beam with a Gaussian intensity profile was studied by the *Z*-scan technique.[8] A schematic illustration of the experimental setup is shown in Fig. 1B. A lens with the focal length $f = 15$ cm focused the laser beam onto the sample. The Gaussian beam waist in the focal plane was $2\omega_0 \approx 75\ \mu$m at $1/e^2$ intensity. To control the input intensity we placed a variable attenuator before the lens. The sample was mounted upon a translation stage and was displaced along the direction of beam propagation.

A screen with a small aperture was placed behind the sample at distance much larger than $2f$ from the lens. The light intensity transmitted through the aperture was measured by a photodetector as a function of the sample's position with respect to the focal plane. This geometry should satisfy two requirements: (1) the distance between the sample and the aperture must be larger than the confocal parameter $z_0 = k\omega_0^2/2$ (here $k \approx 1.18 \times 10^5\ \mathrm{cm}^{-1}$ is the wave number of the green light used in the present experiment) and (2) the sample thickness must be much smaller than z_0. With a distance from the sample to the screen of ~2 m, confocal parameter $z_0 \approx 3.32$ cm, and sample thickness $l = 4$ mm, these requirements were perfectly met. For the beam diameter on the screen, $2\omega_a \approx 7.8$ mm, aperture diameter $2r_a \approx 1.5$ mm ensured low transmittance, $T = 1 - \exp(-2r_a^2/\omega_a^2) \approx 0.07$, which was small enough that a close-aperture on-axis approximation of the *Z*-scan theory[8] could be used in fitting to experimental data.

One extra function that *Z*-scan geometry offers is the detection of nonlinear absorption (the dependence of absorption coefficient α on light intensity). To check the nonlinear absorption we removed the small aperture to make the angular aperture at the detector large enough to collect whole transmitted beam and small-angle scattering.

B. Dynamic Hologram Recording

In dynamic hologram recording, first we measured the intensity dependence of the diffraction efficiency; the intensity of the recording beams was attenuated gradually, with the calibrated neutral-density filters placed in front of the beam splitter. The result is shown in Fig. 2 on a log–log plot. The dependence obeys the second power law for low intensity, but it tends to be saturated at higher intensity. The result indicates that for moderate intensity of the recording light the refractive-index change is directly proportional to the intensity of the light; i.e., the crystal behaves as a medium with third-order frequency-degenerate nonlinearity. The dependence of the diffraction efficiency on beam ratio was also measured, and the result is shown in Fig. 3. The total intensity of two recording waves was kept nearly constant in this experiment and was ~2 W/cm^2. The small (less than 10%) deviation from the mean value did not influence experimental data because for 2-W/cm^2 recording intensity the diffraction efficiency was already saturated on intensity (see Fig. 2). The bell-shaped dependence curve was obtained centered at the recording beam's intensity

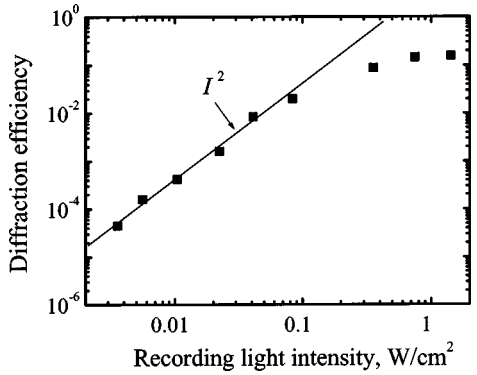

Fig. 2. Dependence of diffraction efficiency on the intensity of recording beams measured with a reading red beam. Solid curve, I^2 dependence. The intensity ratio of the recording green beams is $m = 1{:}2$.

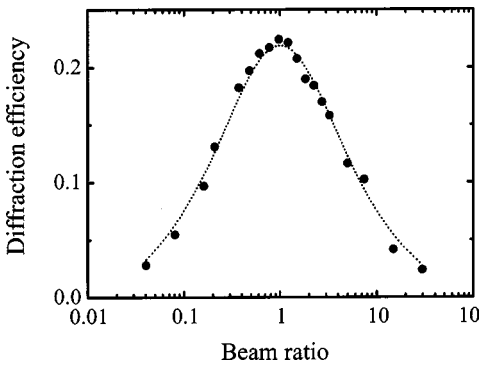

Fig. 3. Dependence of diffraction intensity on beam ratio. The total recording beam intensity is 2 W/cm^2; the recording beam angle is 10° in air. Dotted curve, best fit of the calculated dependence $4m/(1 + m)^2$ to the experimental data; m is the beam ratio.

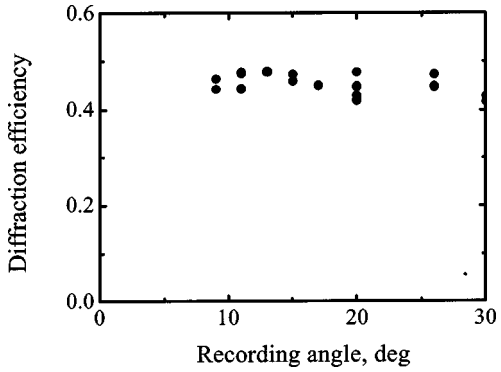

Fig. 4. Diffraction efficiency versus recording angle, measured with green light. The total intensity of the recording waves is 2 W/cm^2.

ratio $m = 1$, as expected for a medium with a local nonlinear optical response. The dotted curve represents the fit, as discussed below.

Diffraction efficiency η does not depend on spatial frequency within the experimental error, as it is shown in Fig. 4. In this experiment the steady-state diffraction efficiency was measured with one of two recording waves ($\lambda = 0.53$ μm) with the other wave blocked. The total intensity of the recording waves was 2 W/cm^2, and the intensity ratio was close to 1:1. Additional experiments proved that the reflection gratings can be also recorded in CdF_2:Ga, Y with a diffraction efficiency comparable to that for transmission gratings. For small recording angles, η was found to be independent of the azimuth angle of linear polarization, provided that the two beams were polarized parallel.

The dynamics of a typical writing–erasure cycle are shown in Fig. 5. The total intensities of the two recording beams in Figs. 5A and 5B are ≈0.1 and ≈1.0 W/cm^2, respectively. The signal-to-noise ratio is still acceptable, as the intensity of recording light is decreased by nearly 3 orders of magnitude. For small intensities (and therefore for small diffraction efficiencies) the background scattered light was subtracted before the standard decay and buildup dependences we fitted. It should be noted that for intensities larger than 1 W/cm^2 the dynamics of grating recording show an easily detectable transient peak (Fig. 5B).

To extract the data on temporal variation of the refractive index we plotted the square root of the diffracted wave's intensity in Figs. 6A and 6B for the processes of decay and buildup, respectively. The solid curves represent the best exponential law fit to the measured data. From the fitting, the characteristic buildup time was extracted; it is shown in Fig. 7 as a function of the intensity of the recording light.

The dynamics of the grating buildup allow for the evaluation of holographic sensitivity S, defined as

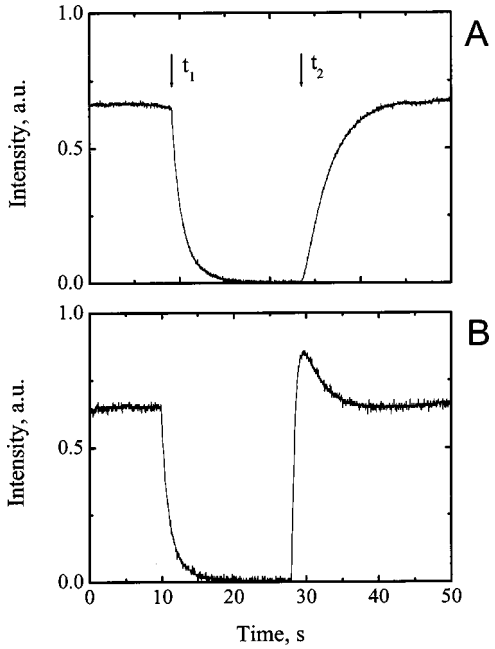

Fig. 5. Temporal evolution of the diffraction efficiency when the recording green light is stopped at $t = t_1$ (grating decay) and when it is switched on at $t = t_2$ (grating buildup). The total intensities of the recording beams are ~0.1 and ~1.0 W/cm^2 for A and B, respectively.

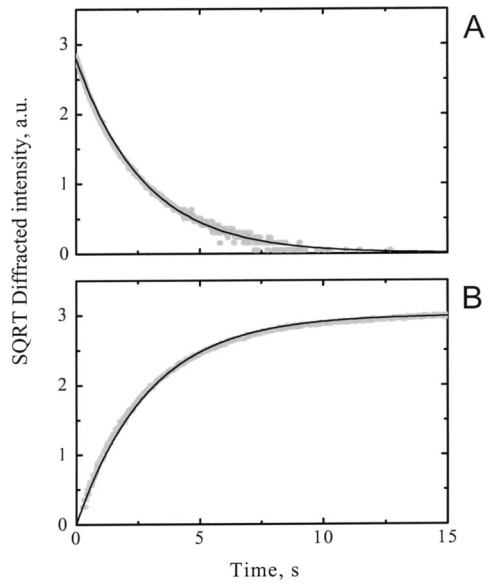

Fig. 6. Temporal variation of the square root of diffraction efficiency for A, grating decay and B, grating buildup. Solid curves, best exponential fits. The total intensity of the recording beams is 1.5 mW/cm^2.

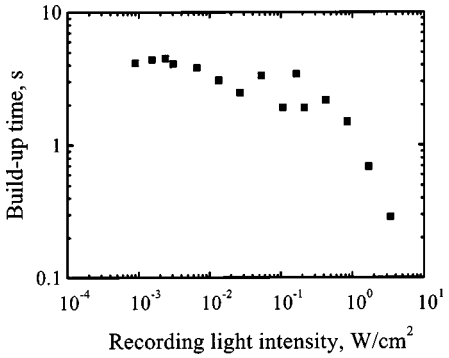

Fig. 7. Grating buildup time versus recording beam intensity.

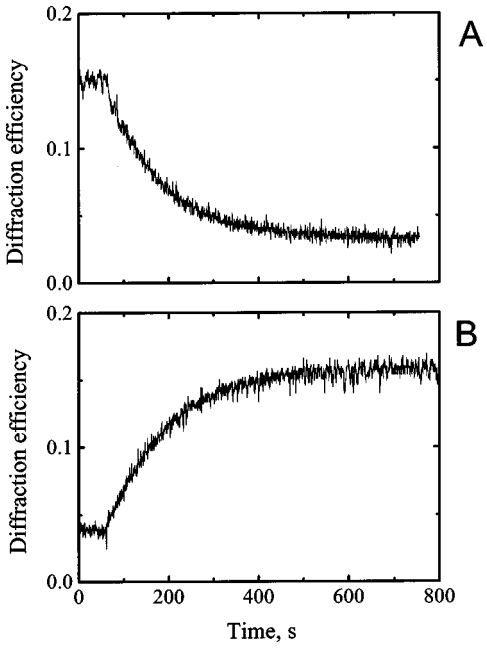

Fig. 8. Temporal variation of diffraction efficiency when 1.06-μm irradiation A, starts to illuminate the CdF_2:Ga, Y sample and B, is switched off.

$$S = \frac{1}{I_0 l}\frac{d\sqrt{\eta}}{dt}\bigg|_{t=0}, \tag{2}$$

where I_0 is the total intensity of the recording beams and l is the sample's thickness (see, e.g., Refs. 10–12). The sensitivity evaluated from the data of Fig. 6 is $S \approx 4$ cm/J.

To study the possible influence of near-infrared radiation on the recording and erasure processes we directed one more Nd^{3+}:YAG laser beam (λ=1.06 μm, 200 mW) to the CdF_2 sample at nearly normal incidence. That beam was adjusted to intersect the recording beams inside the sample. The intensity of infrared light at the input face of the sample was $\approx$5 W/cm^2; the intensity of the recording green light was $\approx$1 W/cm^2. This auxiliary illumination caused a gradual decrease of the grating efficiency, as shown in Fig. 8A. Note that the phenomenon was observed on quite a larger time scale than the process illustrated in Fig. 6. The inhibition of the recording process caused by infrared radiation was reversible. When 1.06-μm radiation was switched off, the diffraction efficiency returned to its initial value, as shown in Fig. 8B.

Finally, the holographic recording of binary two-dimensional images was tested in CdF_2:Ga, Y at room temperature. A standard U.S. Air Force resolution chart was used as a transparency. The incident laser beam was expanded such that the divergent beam, with a diameter of $\sim$5 cm, illuminated the resolution chart. A lens with a 15-cm focal length was used to form the image behind the sample, which was placed close to the plane of the largest confinement. To ensure good intersection of the beams and homogeneity in intensity distribution, the diameter of the reference beam was 2 times larger than that of the object beam inside the crystal. The reference beam's power was adjusted to be 100 times larger than the power of the signal beam; the total power was $\sim$8 mW. The reference beam made an angle of 15° with the object beam in air. Figure 9A shows the initial image of the resolution chart transmitted through the sample, and Fig. 9B shows the image reconstructed from the hologram.

C. *Z*-Scan Experiment

With the same CdF_2:Ga, Y sample and the same laser source, *Z*-scan experiments were performed. Figure 10 represents the dependence of normalized intensity T on the sample's displacement z/z_0 from the focal plane, where z_0 is the confocal parameter. T is normalized with respect to the sample's transmittance T_0. Filled squares show the experimental results measured with 6.6-μW input irradiance; the solid curve represents the best fit of theoretical dependence to the experimental points:

$$T \cong 1 - \Delta\Phi_0 \frac{4(z/z_0)}{[(z/z_0)^2 + 9][(z/z_0)^2 + 1]}, \tag{3}$$

calculated within a small phase-modulation limit (the on-axis phase shift at focus, $|\Delta\Phi_0| < \pi$).[8] The distance z_{p-v} that separates the largest intensity (peak) and the smallest intensity (valley), $z_{p-v} \approx 1.8 z_0$, is close to the theoretical value of $z_{p-v} \approx 1.7 z_0$, which is typical for all $\chi^{(3)}$ materials.[8] The largest measured intensity corresponds to $z/z_0 < 0$, which means that a Gaussian light beam creates a diverging lens; i.e., the refractive-index change is negative in CdF_2:Ga:Y, $\Delta n < 0$ (in agreement with the prediction of Ref. 4).

With increasing input intensity, the contrast of the *Z*-scan T_{p-v}, i.e., the difference between the largest and the smallest transmittances, increased linearly with in-

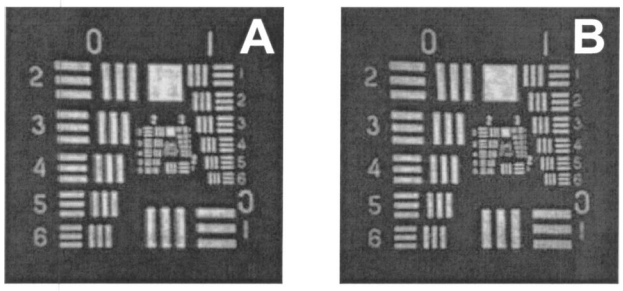

Fig. 9. A, Image of the resolution chart transmitted through the sample and B, image reconstructed in the same plane by diffraction from the dynamic hologram in CdF_2:Ga, Y.

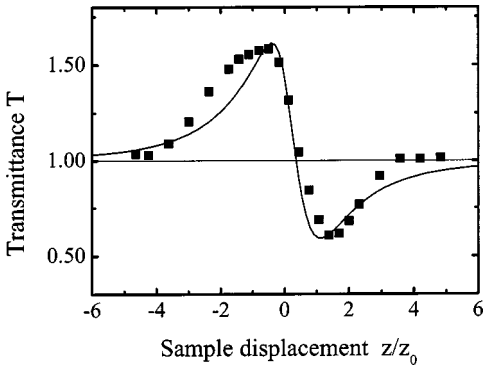

Fig. 10. Transmittance measured by the detector behind an aperture versus normalized displacement from the focal plane of lens L (Fig. 1B). Solid curve, best fit of theoretical dependence [Eq. (3)] to the experimental points; incident beam power, 6.6 μW.

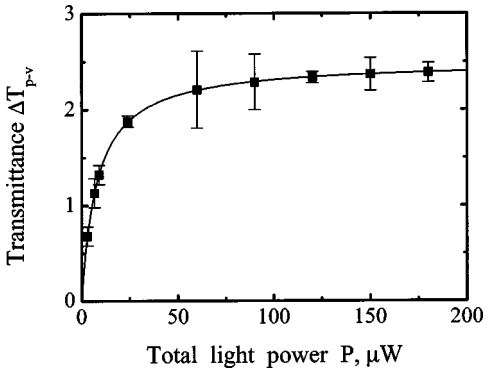

Fig. 11. Transmittance ΔT_{p-v} at maximum (peak) and minimum (valley) versus input power. The solid curve is drawn as a guide to the eye.

put power and was saturated above 30 μW, as shown in Fig. 11. For this intensity range the phase modulation induced in the sample became so large that a characteristic ring structure instead of a Gaussian intensity distribution was observed on the screen.

Without the aperture in front of the detector, the dependence of transmitted intensity on longitudinal displacement of the sample manifested a well-pronounced attenuation in the vicinity of the focal plane. This fact indicates the increase of absorption for high intensity.

3. DISCUSSION

The light-induced refractive-index variation in semiconductor CdF_2:Ga is attributed to the conversion of the DX center from its ground (two-electron, deep) Ga^{1+} state into the metastable (shallow donor) state, in which an electron is weakly bound at the hydrogenic orbital centered at the Ga^{+3} ion.[4–6] The photogenerated weakly bounded electrons affect the sample plasma's frequency in way similar to that of free carriers,[13,14] and therefore a high-frequency dielectric constant becomes modified. The photoinduced changes in refractive index Δn are proportional to the total density of hydrogenic states N_{sh}^0 and should increase with the square of the wavelength[3]:

$$\Delta n = -\frac{2\pi N_{sh}^0 e^2}{n m^* \omega^2} = -\frac{N_{sh}^0 e^2 \lambda^2}{2\pi c^2 n m^*}. \quad (4)$$

Here m^* is the polaron mass, e is the electron charge, and c is the velocity of light.

To calculate a saturated value of the density N_{sh}^0 we propose to use a rate-equation approach (see Refs. 5 and 6), in which linear excitation of the shallow states and both nonlinear (two particles) and linear depopulation are taken into account. It is well known that the steady-state density N_{sh}^0 increases linearly with the pump intensity if both excitation and depopulation are linear processes or if both are quadratic (e.g., two-photon excitation and two-particle recombination).[14] Analysis of the temporal dynamics is of importance for distinguishing between these two possible cases: exponential decay is typical for linear depopulation, whereas one should observe hyperbolic decay for the two-particle process.

Our experimental data indicate that at room temperature the excitation of the shallow states in CdF_2:Ga, Y occurs through linear absorption, whereas their depopulation is a linear relaxation. This can be stated because refractive-index change Δn (and therefore the density of populated states N_{sh}^0) increases linearly with the intensity of the recording light (Fig. 2) and the buildup and decay of Δn and of N_{sh}^0 are close to exponential (Fig. 5). This result does not contradict the model developed in Refs. 4–6 that predicts a hyperbolic-cotangent type of relaxation temporal dynamics, which converts into a simple exponential dependence at high temperatures or in the latest stages of decay.

One more experimental observation, i.e., the dependence of the characteristic buildup time on intensity, can be explained qualitatively within the theoretical model. The analysis of Ref. 6 predicts that at high temperatures the buildup rate will be nearly independent of the intensity of light for small intensities and will increase linearly with intensity for high intensities [Eqs. (11) and (12) of Ref. 6]. This prediction fits well the measured intensity dependence of the refractive-index buildup time[6] (Fig. 7). The characteristic time decreases substantially only at rather high intensities of the recording beams. It should be mentioned, however, that crystal heating by laser light also contributes to faster grating relaxation at high intensities, as is discussed below.

It is necessary to underline that high temperature for the authors of Ref. 6 means a temperature at which thermal depopulation of the shallow state is efficient. With the lifetime of the shallow state limited to a few seconds, we can state that the ambient temperature at which all our experiments have been made just corresponds to the definition of high temperature in Ref. 6.

According to Ref. 6, the shallow-state decay time that is responsible for the buildup and decay times of Δn is strongly temperature dependent. This is why heating of the sample by the recording light may affect the recording process. With the absorption on the level of $\alpha l \approx 0.3$, nearly one third of the incident beam power is pumped into the sample, which can easily result in heating of a sample exposed to 200-mW light to 5 °C above room temperature. With activation energy $\Delta E \approx 0.8$ eV for the

decay time of the photoinduced shallow center concentration,[6] such heating will result in an ≈1.7 times decrease in the characteristic lifetime and in a nearly 3 times decrease in the diffraction efficiency.

Another argument in favor of refractive-index limitations that are due to sample heating by laser light comes from the slow dynamics of the diffraction efficiency variations that we attribute to temperature variation. With the thermal diffusivity $D_{th} \approx 0.035\ cm^2/s$ that is typical for fluoride crystals, the time needed for heat relaxation in a 7-mm-thick sample is only a fraction of second. At the same time, heat exchange with a crystal holder and air is a much slower process, and it may take several tens of seconds to heat a 0.08-cm^3 sample with a 0.2-W laser beam until saturation.

Thus one can expect modifications of the recording and erasure processes that are due to the rise or decrease of the sample temperature, whereas the thermal process of grating recording is completely ineffective with cw recording laser light. The dynamics of temperature variation of the sample exposed to green laser light was measured directly with a thermocouple fixed at a nonilluminated side face of the sample. With a 200-mW unfocused laser beam the sample temperature increased by 4 °C in a characteristic time $\tau_{heat} \approx 30$ s. These results are in agreement with our estimates; they confirm also the possible effect of heating on the recording data.

Heating time $\tau_{heat} \approx 30$ s is obviously larger than the characteristic time of nonlinearity, which is due to the presence of shallow DX centers in CdF_2, $\tau_{sh} \leqslant 3$ s. As a consequence, after the beginning of exposure the diffraction efficiency will reach its steady-state value close to that for an unheated sample within a time interval of few τ_{sh}. With longer exposure the sample temperature will increase until thermal equilibrium is reached, and grating efficiency will drop to a new steady state, which is typical for elevated temperatures. In such a manner the appearance of a transient peak in Fig. 5B can be explained. The slow variations of the diffracted signal when auxiliary illumination is switched on or switched off (Fig. 8) within a scale comparable to τ_{heat} and much longer than τ_{sh} allow us to attribute the detected sensitivity to infrared light to sample heating, too.

Finally, our measurements allow us to deduce the nonlinear constants for CdF_2:Ga, Y. The diffraction efficiency of a uniform three-dimensional phase grating can be described by Kogelnik's formula[7]

$$\eta = \sin^2\left(\frac{\pi \Delta n l}{\lambda}\right). \tag{5}$$

Using Eq. (5), we can evaluate refractive-index change Δn from the data of Fig. 4. For an intensity of the recording waves of ~1 W/cm^2 and $m = 1$, η is ~0.5 and the estimated ultimate refractive index change is $\Delta n \approx 0.3 \times 10^{-4}$.

For unequal intensities of the recording beams the refractive-index change in Eq. (4) will be directly proportional to the fringe contrast.[7] The solid curve in Fig. 3 represents the best fit to calculated dependence $4m/(1+m)^2$ when the $\sin^2$ term can be replaced by the second power law. The reasonable agreement with the experimental results indirectly confirms the dependence of the refractive-index change on linear intensity.

From the dynamics of diffraction efficiency, sensitivity to grating recording has been evaluated. The value obtained, $S \approx 4$ cm/J, is much larger than that which is typical for the classic photorefractive crystal $LiNbO_3$:Fe ($S \approx 0.02$–0.07 cm/J) and is comparable with that for sillenites such as $Bi_{12}TiO_{20}$ ($S \approx 10$ cm/J),[15] but it is still smaller than sensitivity of Polaroid photopolymer ($S \approx 20$ cm/J).[11] This comparison is, however, not completely correct because at room temperature CdF_2 exhibits a rather short storage time, whereas $LiNbO_3$:Fe and Polaroid photopolymer ensure recording of permanent holographic gratings. A more suitable characteristic of CdF_2 would be a nonlinear susceptibility[12] $\chi^{(3)}$, which can be evaluated from data similar to those presented in Fig. 2 but measured with green light, $\chi^{(3)} \approx 1.4 \times 10^{-10}\ m^2/V^2$.

It is impossible to deduce the sign of $\chi^{(3)}$ from measurement of η because η is proportional to the square of the refractive-index change.[6] This sign of $\chi^{(3)}$ was determined to be negative by a *Z*-scan experiment in which self-defocusing was observed, as explained in Subsection 3.C of this paper. The *Z*-scan experiment could also be used for evaluation of $\chi^{(3)}$. Special care should be taken, however, in interpreting these data because of the large difference in light intensities in the two techniques.

ACKNOWLEDGMENTS

This study has been supported by the International Science and Technology Center (project 2136). S. Odoulov is grateful to the Japan Society for the Promotion of Science for an invitation fellowship. S. Odoulov and K. Shcherbin cordially thank their colleagues from the Nonlinear Optics Laboratory of Waseda University for their hospitality. We are grateful to the reviewers for valuable remarks and suggestions.

S. G. Odoulov's e-mail address is odoulov@iop.kiev.ua.

REFERENCES

1. J. M. Langer, "DX-like centers in solids (metastability, bistability and negative-U)," Rev. Solid State Sci. **4**, 297–317 (1990).
2. A. I. Ryskin and P. P. Fedorov, "Donor impurities and DX centers in the ionic semiconductor CdF_2," Phys. Solid State **39**, 943–947 (1997).
3. A. I. Ryskin, A. S. Shcheulin, B. Koziarska, J. M. Langer, A. Suchotski, I. I. Bushinskaja, P. P. Federov, and B. P. Sobolev, "CdF_2:In: a novel material for optically written storage of information," Appl. Phys. Lett. **67**, 31–33 (1995).
4. A. I. Ryskin, A. S. Shcheulin, E. V. Miloglyadov, R. A. Linke, I. Redmond, I. I. Bushinskaja, P. P. Federov, and B. P. Sobolev, "Mechanism for writing and decay of holographic gratings in semiconducting CdF_2:Ga," J. Appl. Phys. **83**, 2215–2221 (1998).
5. S. A. Kazanskii, A. A. Ryskin, A. S. Shcheulin, R. A. Linke, and A. E. Angervaks, "DX center gratings in real-time holography," Physica B **308–310**, 1035–1037 (2001).
6. R. A. Linke, A. S. Shcheulin, A. I. Ryskin, Bushinskaja, P. P. Federov, and B. P. Sobolev, "Properties of CdF_2:Ga as a medium for real time holography," Appl. Phys. B **72**, 677–683 (2001).

7. R. J. Collier, Ch. B. Burckhardt, and L. H. Lin, *Optical Holography* (Academic, New York, 1971).
8. M. Sheik-Bahae, A. A. Said, T.-H. Wei, D. J. Hagan, and E. W. Van Stryland, "Sensitive measurement of optical nonlinearities using a single beam," IEEE J. Quantum Electron. **QE-26**, 760–769 (1990).
9. P. P. Federov, I. I. Bushinskaja, S. P. Ivanov, B. P. Sobolev, A. S. Shcheulin, and A. I. Ryskin, "A new class of holographic materials based on semiconducting CdF_2 crystals with bistable centers. II. Growth of optically perfect crystals," Opt. Spectrosc. **92**, 133–140 (2001).
10. A. Adibi, K. Buse, and D. Psaltis, "Sensitivity improvement in two-center holographic recording," Opt. Lett. **25**, 539–541 (2000).
11. R. M. Shelby, "Media requirements for digital holographic storage," in *Holographic Data Storage*, H. J. Coufal, D. Psaltis, and G. T. Sincerbox, eds., Vol. 76 of Springer Series in Optical Science (Springer-Verlag, Berlin, 2000), pp. 101–111.
12. P. N. Butcher and D. Cotter, *The Elements of Nonlinear Optics* (Cambridge U. Press, Cambridge, 1990).
13. J. P. Woerdman, "Formation of a transient free carrier hologram in Si," Opt. Commun. **2**, 212–217 (1970).
14. H. J. Eichler, P. Gunter, and D. Pohl, *Laser Induced Dynamic Gratings* (Springer-Verlag, Berlin, 1986).
15. M. P. Petrov, S. I. Stepanov, and A. V. Khomenko, *Photorefractive Crystals in Coherent Optical Systems* (Springer-Verlag, Berlin, 1991).